Trans-Dimensional multimode surface wave inversion of DAS data at CaMI-FRS

Luping Qu, Jan Dettmer and Kris Innanen

ABSTRACT

Inversion of surface wave seismic data to aid in the characterization of the near-surface is a rich and well-explored field. However, several new areas of technology development, both algorithmic and acquisition-based, have the potential to lead to significant improvements in the accuracy and availability of near-surface models. To this end, in this study we apply a trans-dimensional surface wave dispersion inversion, which incorporates jointly using the multimodal phase velocity information of the Rayleigh wave, and we apply it to Distributed Acoustic Sensing (DAS) data acquired with a trenched fibreoptic cable. The joint use of multiple modes, combined in a stochastic sense, is explained in detail in this work. A thorough spectral analysis and error estimations on DAS data are required, and in processing the data we have found that a new mode separation method, called dispersion compensation, permitted clear picking of dispersion curves. Multimodal phase velocity dispersion curves are extracted from the densely sampled DAS data, and then used as input to a multimode phase velocity trans-dimensional inversion. We examine the subsurface phase velocity model recovery, and in particular show that better-resolved models result from the incorporation of the higher. Both synthetic and field testing are carried out, the latter involving DAS data acquired at the Containment and Monitoring Institute-Field Research Station as an offshoot of the CREWES 2018 mulit-offset multi-azimuth VSP experiment. Synthetic models appear to be consistent with our theoretical expectations, and results of real data furthermore appears to be in excellent agreement with known geology features. A better characterization of shallow area is revealed compared with other research results.

INTRODUCTION

CREWES is developing practical elastic and multicomponent seismic waveform inversion methodologies which are maximally flexible and applicable to monitoring of conventional and unconventional onshore reservoirs (or ocean-bottom monitoring in offshore settings). In practice these EFWI algorithms when applied to land data require very careful management of surface wave modes to have been carried out. Furthermore specific applications of near-surface seismic methods within (e.g.) geohazard assessment will tend to benefit from an expansion of the toolbox for developing robust models in the shallowest 10-100m of the Earth involving new algorithms and acquisition techniques. Motivated by all this, in this paper we present results of an application of a global, transdimensional inversion approach to surface wave data, focusing on use of fibreoptic (DAS) data. In an associated report, Cova and Innanen (2019) analyze the application of elastic FWI to similar single- and multimode data. The novelty of this paper is threefold: (1) the application of the transdimensional inversion, to (2) multimode data, acquired (3) from a fibreoptic/DAS system.

Inversion of surface-wave dispersion inversion

Dispersion of surface waves is observed for both Rayleigh and Love waves in the presence of stratification with increasing shear-wave velocity as a function of depth (Haskell, 1953; Takeuchi and Saito, 1972). As a result, dispersion curves can be extracted for both Rayleigh and Love waves and these curves contain information about the subsurface shear-wave velocity structure. Dispersion curves are commonly inverted to infer shear-wave velocity information (Xia et al., 1999; Rix et al., 2001). Here, we apply surface-wave dispersion (SWD) inversion to gain knowledge about the weathering layer. This knowledge is important for static corrections and prior information for waveform inversion (e.g., starting models) in exploration seismology (Dulaijan and Stewart, 2010). However, several challenges are encountered in SWD inversion which are addressed here by a Bayesian inversion approach. The quantitative characterization of the model parameters is addressed by Bayesian inversion approach. The selection of the model size (underground layer number) is flexibly solved through trans-Dimensional inversion. The influence of data noise on inversion results and data error estimations are settled using hierarchical error models. In all these aspects, the trans-Dimensional Bayesian inversion method has performed as a proper and powerful tool to obtain shear wave velocity structure in shallow sites. Compared with linear inversion methods, biased and erroneous solutions generated from subjective regularization and incorrect priors can be avoided. The crucial challenge in stochastic SWD inversion is the solution non-uniqueness due to the limited information contained in the dispersion curves, which is also the reason for the difficult characterizations of other model parameters like P wave velocity and density. Since the non-uniqueness can be reduced by determination of layer number and layer thickness information, other complementary data type such as receiver functions and refraction waves helping with stratification can be incorporated to add more constraints on the solutions. But if there is no other data resource, higher mode phase velocities and group velocities extracted from the present data can also be utilized to provide more information about the underground.

The result improvements brought by higher mode dispersion curves are effectively proved in previous research (Pan et al., 2018; Li et al., 2012; Feng et al., 2005). For the higher mode dispersion curves, higher frequency coverage range and deeper penetration can enhance the shallow and deep resolution separately. Finally, the uncertainty at all depths will be reduced. All these study results and the shortage of other available data types impel us to conduct a surface wave inversion utilizing multimodal phase velocity. One basic issue needs to be figured out here is the joint of multimode dispersion curves in the stochastic sense. In linear inversion, multimode inversion misfits can be the weighted summation of fundamental mode and higher order modes (Luo et al., 2007). In non-linear inversion, for example, Bayesian inversion, researches have been done with efficient calculation of higher mode dispersion curves (Maraschini et al., 2010). But more clear explanations of how to implement multimode inversion in Bayesian inversion should be given. Another preliminary problem in multimode inversion is the mode separation. Fundamental mode is relatively easy to pick as its energy is dominant and continuous, while higher modes usually couple together. High resolution Radon transform (Luo et al., 2009) has been used to provide a better display of different modes. However, keeping fundamental mode and higher modes in the same spectrum and applying normalized display may still interfere the full presentation of both fundamental mode and higher modes. A new way for mode

separation named dispersion compensation method is used (Xu et al., 2012), which could separate multimodal dispersion curves effectively.

DAS data and CaMI site

Distributed Acoustic Sensing (DAS) is a novel technology for collecting geophysically meaningful data. Since it was born, DAS has drawn abundant attentions in geophysical exploration due to its great application potentials and salient advantages: nonintrusive, low-cost and dense sampling. In DAS acquisition, the interrogator unit can record the small vibrations of imperfections result from the localized acoustic energy through the backscattering measurements. The measurements of backscattering will be related to fibre deformation involving the wavefield variations in local regions. Theoretically, the interrogator is sensitive to the movement of imperfections parallel to the fibre orientation, but not sensitive to particle movements in other directions. Therefore, in straight line surface DAS acquisition, this character limits its application for reflection or refraction wave data processing, but makes it a perfect recording system for surface waves. Daley et al. (2013) compared the horizontal and borehole geometry records, further confirmed that the signal to noise ratio is too low for body wave observation as the incidental reflected angle is comparatively small. However, one problem worth considering in surface DAS data is the coupling of Rayleigh wave and Love wave in seismograms. When the source is not located in line with the sensing fibre, the record of the horizontal motion could be the coupling horizontal components of Rayleigh wave and Love wave. They could be decoupled with multicomponent receivers or additional information, but there is no way to decouple them with only one component recording in surface DAS fibre. The field data we use is in an inline geometry, thus, the coupling of Rayleigh waves and Love waves is negligible. But it is still an important field for further study.

To date, most geophysical study on DAS has been implemented in boreholes for seismic profiles, flow monitoring and temperature measurements (Clarke and Sandberg, 1983; Cox et al., 2012; Daley et al., 2013; Krohn et al., 2014; Mateeva et al., 2014). There are only several studies on surface DAS acquisitions (Daley et al., 2013; Hornman, 2017). Thus, a thorough research of surface DAS in active source experiments is needed. The densely sampled DAS data should be utilized to obtain a better characterization of near surface.

The Field Research Station (FRS) is near the town of Brooks in the Newell County which is approximately 200km southeast of Calgary. The survey developed by Containment and Monitoring Institute (CaMI) involved data acquisition of GPS, interferometric synthetic aperture radar (InSAR), hydrology, microseism, microgravity, electrical resistivity, passive source seismology, and active source seismology (Lawton et al., 2017). These data were collected initially to improve understandings and technologies for geological containment and storage of CO_2, monitoring of fossil fuel production and environmental mitigation. In this study, active source data collected over 1km DAS fibre is used for near surface investigation through surface wave dispersion inversion. In this study, joint inversion of multimodal Rayleigh wave phase velocity and group velocity is implemented both on synthetic data and DAS data. The non-unique solutions inferred by phase velocity and group velocity are analyzed separately. An advanced mode separation method is adopted on the

real data. Improved joint inversion results are shown, while the feasibility of DAS data for SWD inversion is revealed.

THEORY

This part illustrates the principle for dispersion compensation, multimode likelihood formulation, trans-Dimensional SWD inversion and data error estimation.

Dispersion compensation

To conduct multimode surface wave inversion on real data, one preliminary problem is mode separation. Sometimes, different mode dispersion curves, especially higher modes are very close, which may cause error in phase velocity picking. Incorrect observing data then lead to unreliable inversion results. Therefore, an effective mode separation method should be used to pick dispersion curves accurately. Here, a method called dispersion compensation is adopted to conduct mode separation (Xu et al., 2012). The multimodal Rayleigh wave data can be treated as the response of a broadband source F(ω). The dispersive phenomenon can be treated as a phase shifting of a constant velocity propagation. Therefore, the multimode surface wave $S(\omega)$ in frequency domain at a certain offset x could be expressed as

$$S(\omega) = \sum_{i=1}^{N} Amp_i T_i(\omega) F(\omega), \tag{1}$$

where $T_i(\omega) = \exp(-jk_i(\omega)x)$,$k_i(\omega)$ is the dispersion phase shifting from original signal. Amp_i is the amplitude for each mode. The dispersion could be reversed by dispersion compensation, which is done through a reversed phase shifting. The process can be complemented by multiplying $T_i^{-1}(\omega) = \exp(jk_i(\omega)x)$, which gives

$$S^*(\omega) = T_i^{-1}(\omega)S(\omega) = Amp_i F(\omega) + T_i^{-1}(\omega) \sum_{j=1, j\neq i}^{N} Amp_j T_j(\omega) F(\omega). \tag{2}$$

$S^*(\omega)$ is the frequency spectrum after dispersion compensation. Different velocities $k_i(\omega)$ can be used to implement the dispersion compensation. Then, different modes with diverse dispersive velocities compensated with the same velocity should distribute in different time zones, possessing different slopes. For example, we could compensate for the fundamental mode based on an initial measurement of the fundamental mode phase velocity. After compensation, the fundamental mode will be flatted, and higher modes with different velocities will be overcompensated to the minus time zone in this case. Thus, the fundamental mode could be extracted through window selection. Other modes could also be extracted in the same way. The compensation velocity utilized can be selected from the frequency-velocity spectrum.

Trans-Dimensional SWD inversion

Based on Bayes' rule, the posterior probability density (PPD) is defined as

$$P(\mathbf{m}|\mathbf{d}) = \frac{P(\mathbf{d}|\mathbf{m})\, P(\mathbf{m})}{P(\mathbf{d})}. \tag{3}$$

d is the measured data, which is the dispersion curves picked in the spectrum of observed data. **m** is a random model containing all the model parameters. $P(\mathbf{m}|\mathbf{d})$ is the posterior probability density, which quantifies the model parameters give data $P(\mathbf{d}|\mathbf{m})$ and prior model information. $P(\mathbf{m})$ is the model prior information, which is bounded, uniform distributions in a physically reasonable range for all model parameters. $P(\mathbf{d}|\mathbf{m})$ is data occurrence probability given a certain model. With fixed observing data, $P(\mathbf{d}|\mathbf{m})$ scaled by evidence is also known as likelihood function as is shown in Equation 7. In the likelihood function, data could be treated as the condition of the current model parameters occurrence. As in dispersion surface wave inversion, the non-uniqueness of solutions not only results from the variable combination of model parameter values, but also influenced by uncertain model parameter numbers, which is layer number in SWD inversion. In trans-Dimensional inversions, model parameter number is treated as unknown, and integrated over in a hierarchical Bayesian sense (Dettmer et al., 2010). The uncertainty of layer number will be included in the posterior and examined by the likelihood function. With the incorporation of variant model parameter number k, the posterior could be transformed into

$$P\left(k, \mathbf{m}_k|\mathbf{d}\right) = \frac{P\left(k\right) P\left(\mathbf{d}|k, \mathbf{m}_k\right) P\left(\mathbf{m}_k|k\right)}{\sum_{k' \in \mathcal{K}} \int_{\mathcal{G}} P\left(k'\right) P\left(\mathbf{d}|k', \mathbf{m}'_{k'}\right) P\left(\mathbf{m}'_{k'}|k'\right) d\mathbf{m}'_{k'}}, \tag{4}$$

where k is the layer number while k' is the proposed layer number using birth-death scheme, $P\left(k\right)$ is the prior for this hyperparameter k, which is in a group of fixed dimension spaces $\mathcal{K}$. As the propagator matrix is used to synthetically generate dispersion curves. A partition model or layered model is naturally employed. Correspondingly, a similar Metropolis Hasting acceptance criterion from current model $\mathbf{m}_k$ to a proposed model $\mathbf{m}'_{k'}$ is

$$\alpha = \min\left[1, \frac{P\left(k', \mathbf{m}'_{k'}\right)}{P\left(k, \mathbf{m}_k\right)} \frac{P\left(d|k', \mathbf{m}'_{k'}\right)}{P\left(d|k, \mathbf{m}_k\right)} \frac{Q\left(k, \mathbf{m}_k|k', \mathbf{m}'_{k'}\right)}{Q\left(k', \mathbf{m}'_{k'}|k, \mathbf{m}_k\right)} |\mathbf{J}|\right]. \tag{5}$$

This criterion is utilized to meet the requirement of detailed balance once the model parameter number or values are perturbed. Layer number k is involved in the likelihood $P(d|m)$ and proposal distribution ratios Q. $|\mathbf{J}|$ is the Jacobian of transformation from $(k, \mathbf{m}_k)$ to a perturbed state $(k', \mathbf{m}'_{k'})$. Once a suitable birth-death proposal for k is determined, $|\mathbf{J}|$ could be simplified to 1. Parallel tempering is usually adopted to allow the state exchange between high temperature and low temperature, so that Markov Chains could explore wider and converge more efficiently. For every Markov chain with the starting temperature of T=1, there will be several complementary Markov chains running with higher starting temperatures as assists. Markov chains with higher temperature will explore wider parameter space and have probabilities to exchange the current statement with a Markov chain that explore locally, which will improve the dynamic property of inversion and help find a higher probable region quickly. The acceptance criterion for state exchange of a chain pair is

$$\alpha_{PT} = \min\left[1, \left\{\frac{P\left(d|k', \mathbf{m}'_{k'}\right)}{P\left(d|k, \mathbf{m}_k\right)}\right\}^{\beta_i - \beta_j}\right]. \tag{6}$$

β_n and β_l are annealing parameters. When the Markov Chain starts at temperature=1, β=1. If the starting temperature is larger than 1, β will be less than 1. i and j are two random states for this Markov Chain pair.

Likelihood formulation for multimode inversion

In linear surface wave inversion, multimode inversion misfit is the summation of the 2 norm residuals. While in Bayesian inversion, the multimode inversion should not be summation, as the misfit is the likelihood in essence. In statistics, the probability of two independent events occurring together equals to the multiplication of their likelihoods. As there is no explicit relation between the fundamental mode and the higher modes, we will treat them as independent. Therefore, the likelihood of the model that meets both the fundamental and higher modes of phase velocity dispersion curves is the product of the model likelihoods which fit all those dispersion curves (Li et al., 2012), expressed as

$$L(\mathbf{m}) = \prod_{i=1}^{S} \frac{1}{\sqrt{(2\pi)^{N_i}|\mathbf{C}_{\mathbf{d}i}|}} \exp\left(-\frac{1}{2}\mathbf{r}_i^T \mathbf{C}_{\mathbf{d}i}^{-1}\mathbf{r}_i)\right). \tag{7}$$

i could be the mode index for phase velocities which are used in the inversion process with a total number of S. $\mathbf{r}_i$ is the data residuals between the measured data and the synthetic data. $\mathbf{C}_{\mathbf{d}i}$ is the data covariance matrix for a specific dispersion curve and $\mathbf{m}$ represents all the the model parameters.

Data error treatment

To guarantee the accuracy of inversion, a rigorous estimation of data error must be considered. Ignoring biases and correlations of data error can lead to biased, incorrect model parameter estimations. Therefore, an iterative and nonparametric data error estimation is employed to include the non-stationary error and correlated data errors in the inversion (Dettmer et al., 2007). For a preliminary inversion, the data covariance matrix $\mathbf{C}_d$ is not known. Thus, an independent Gaussian distributed data error with unknown standard deviation can be assumed, which simplifies the data covariance matrix to $\delta^2 I$. Next, a more accurate data covariance matrix could be estimated through the data residuals r. Since the correlated error has already been included in the off-diagonal terms of the matrix, non-stationary error can be included by scaling the Toeplitz matrix into a non-Toeplitz one. The data error estimation procedure for a data with unknown errors is as follows. First, the data error covariance matrix is calculated as the Toeplitz matrix for auto-covariance of data residual r,

$$C_i = \frac{1}{N}\sum_{k=0}^{N-i-1}(r_{i+k} - \bar{r})(r_k - \bar{r}), \tag{8}$$

Here C_i is the new data covariance matrix, i is the element index in the covariance matrix, $\bar{r}$ is the mean for the data residual. k is the index for To include the non-stationary error, first, an ergodic process is assumed and a standard deviation δ_i using data residuals by running rms average over Q data is calculated,

$$\delta_i = \sqrt{\frac{1}{Q}\sum_{k=i-Q/2}^{i+Q/2} r_k^2}. \tag{9}$$

Next, a scaled data residual n_i is obtained by

$$n_i = \frac{r_i}{\delta_i}. \tag{10}$$

Then, a new Toeplitz data covariance matrix $\widetilde{\mathbf{C}_d}$ is calculated using n_i, as expressed in Equation 10. The final non-Toeplitz covariance matrix is calculated by scaling the new Toeplitz covariance matrix with standard deviations

$$C_{ij}^{(d)} = \widetilde{C}_d \delta_i \delta_j. \tag{11}$$

Thus, a data covariance matrix including non-stationary error and correlated error is found. Based on more comprehensive data error analysis, a more accurate characterization of the model parameters distribution could be obtained.

SIMULATION RESULTS

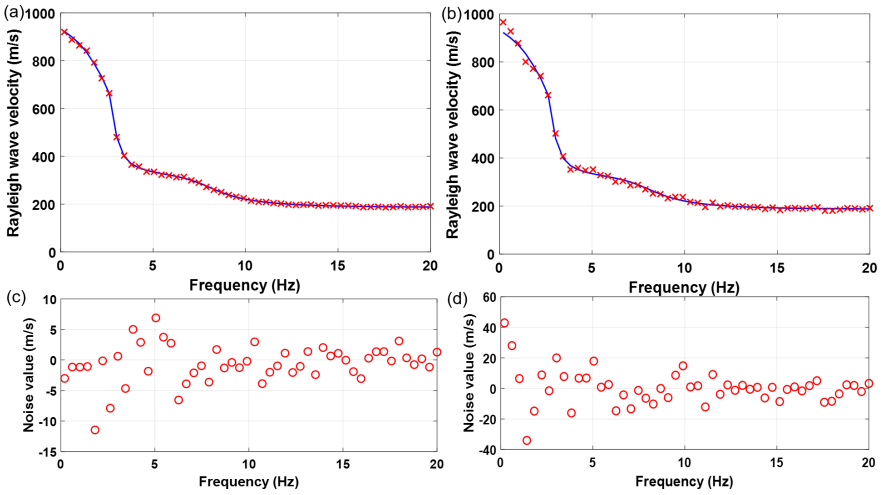

FIG. 1. Observing data for three-layered model with different random noise standard deviation. (a) Observing data (red dot) with 1% random noise and (c) is the corresponding data error. (b) Observing data (red dot) with 3% random noise and (d) is the corresponding data error.

To verify the feasibility of this algorithm, a three-layered simulated model over a half-space is used to apply the inversion process. As for forward modeling, GPDC is used to generate a synthetic dispersion curve. Frequency sampling for this dispersion curve is uniform from 0.2 Hz to 20 Hz, with 50 points totally. Two random data errors with different standard deviations are added to the generated data for inversion at first to examine the influence of data error levels on inversion resolution. The observing data with different data error standard deviations are shown in Figure 1, and the corresponding posterior for these two observing data is shown in Figure 2 and Figure 3. Correlated data error (Figure 4) is generated by multiplying an Gaussian random number array with the Cholesky decomposition of a constructed data error covariance matrix with non-zero decaying off-diagonal terms. Priors for all the variables are uniform within reasonable ranges. As an increasing background velocity is pre-set for better convergence, the posterior we are calculating is actually the perturbation of shear wave velocity (Vs). Here, the prior setting for Vs perturbation is [-200, 500] m/s, for Vp/Vs ratio is [1.4, 10]. Layer number lies in a range from 2 to 30. Minimal thickness is set to be 0.01 m, while the maximal thickness depends on the dispersion curve, which is set to be 90 m for this synthetic model. Twenty cores are used for Markov Chain simulations, in which 5 cores starting from the temperature T=1 are collected for samples, other 15 cores starting with increasing temperatures are used

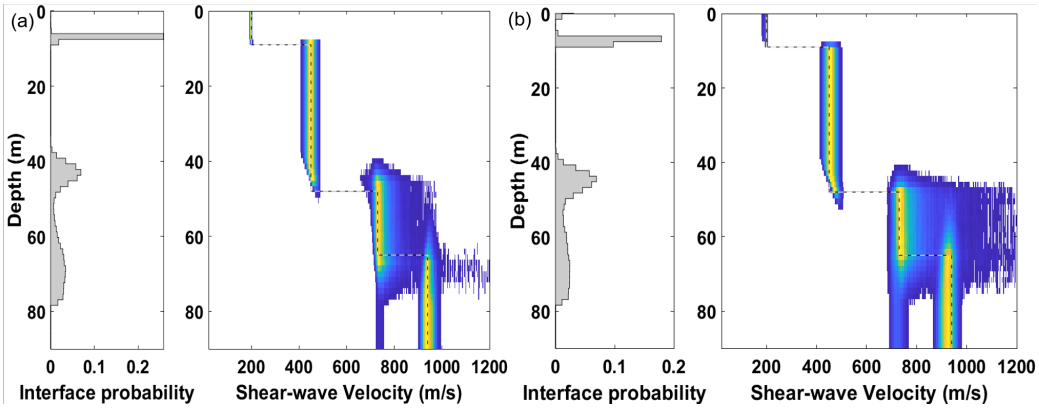

FIG. 2. Posterior for data with different levels of random noise. (a) Results of data with 1% random noise. (b) Results of data with 3% random noise

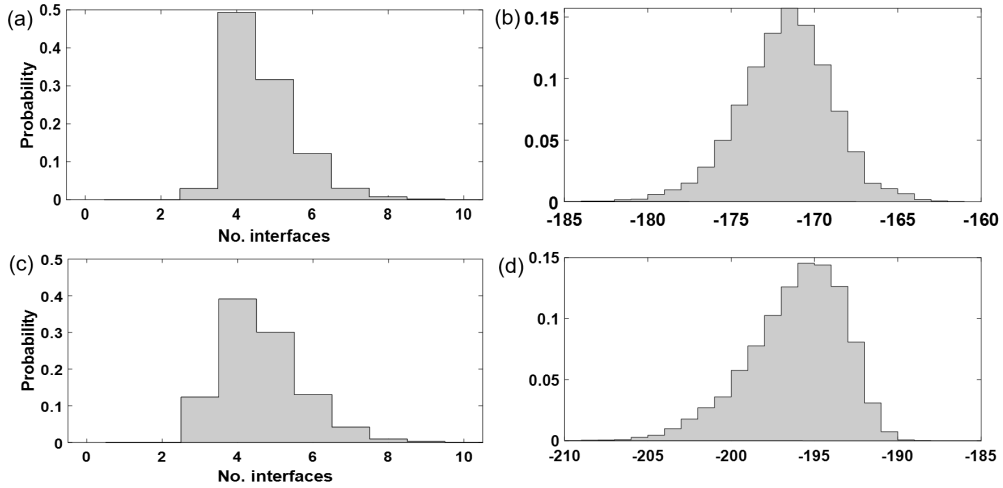

FIG. 3. Posterior layer number distribution and likelihood distribution.(a) Posterior layer number distribution for the synthetic data with 1% random noise. (b) Likelihood distribution for the same data. (c) Posterior layer number distribution for the synthetic data with 3% random noise. (d) Likelihood distribution for the same data.

as complementary. Over 400,000 iterations are computed with convergence guaranteed, and the tailing 100,000 samples are used for statistically calculation. The quality of samples collected can be checked by generating an ensemble of dispersion curves for data fitting. From Vs profile marginals and posterior hist-count in Figure 2, clear layer interfaces are resolved, and model parameter probability distributions match well with the true model.

For a regorious data error estimation, a preliminary inversion assuming data error are independent Gaussian distributed values is conducted. Then, the scaled data covariance matrix involving correlated errors is obtained through the scaling the autocovariance matrix of data residuals(Figure 4). With the new data covariance matrix, subsequent inversions are carried out, which could be an iterative process. In the end, an ensemble of samples collected from the final inversion could be statistically counted. The observing data with correlated error is shown in Figure 4. The posteriors for the preliminary inversion and final inversion process are displayed in Figure 5. It shows ignoring correlated data error could influence the characterization of model parameters. But with cautious estimation of data covariance matrix, results could be improved to a large extent. Dispite the correlated noises

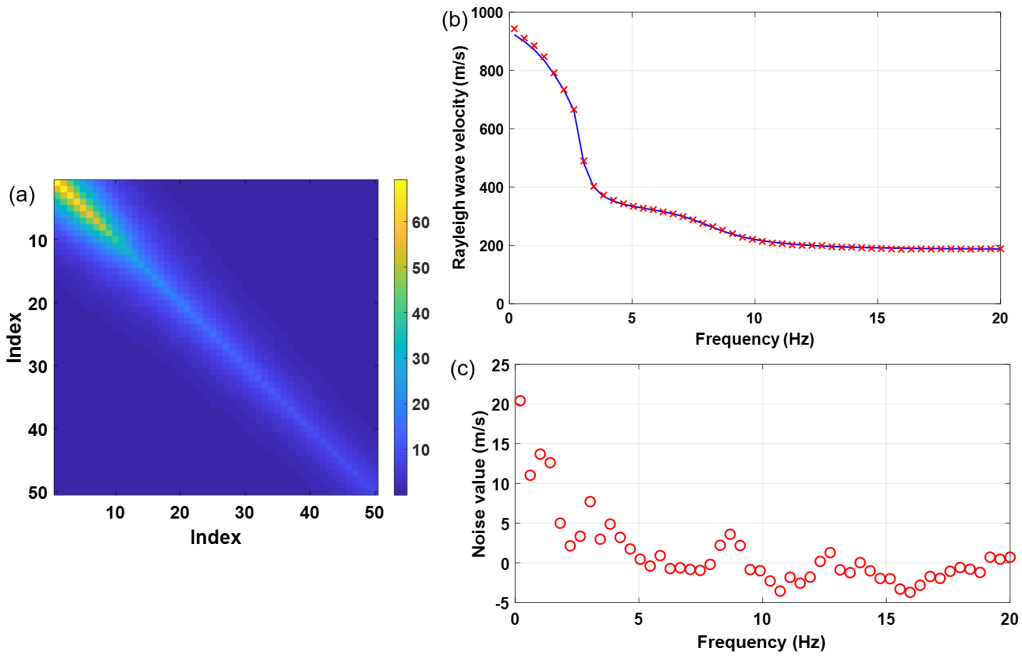

FIG. 4. Observing data with correlated noise. (a) Correlated noise matrix. (b) Observing data (red dot) with true data (blue line). (c) Correlated noise.

on the data, the final posterior shear wave velocities and interfaces are close to the results without correlated noises, and they are both reasonably close to the true model.

Based on the simulated model tests above, not only the model parameters are inferred through trans-Dimensional inversion, different types of data errors are well estimated and inferred The application on synthetic model verifies the robustness and feasibility of this algorithm on layered models.

In addition, a multimode inversion is conducted to be compared with the inversion results obtained with only the fundamental mode. Here, a different model with thinner shallow layers and larger velocity jumps in neighboring layers is used to better demonstrate the

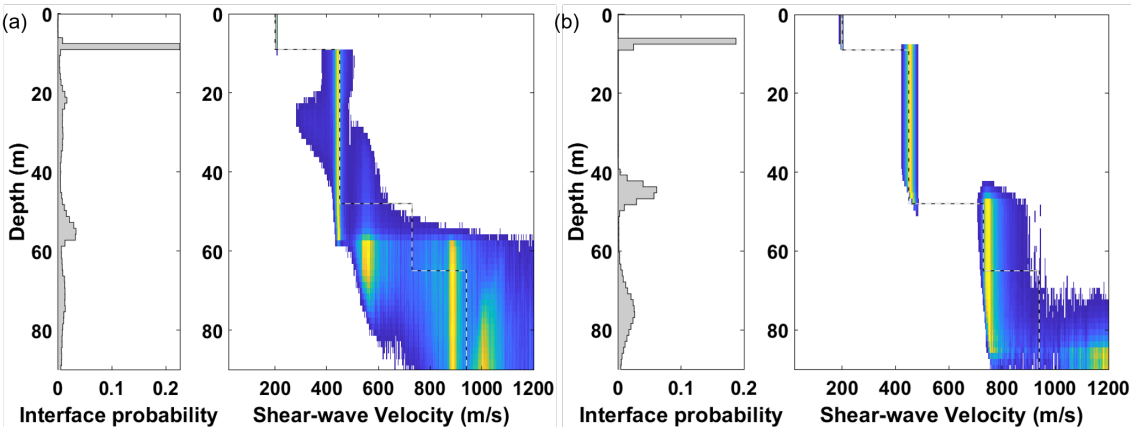

FIG. 5. (a) Result of ignoring correlated noise. (b) Result of involving correlated noise.

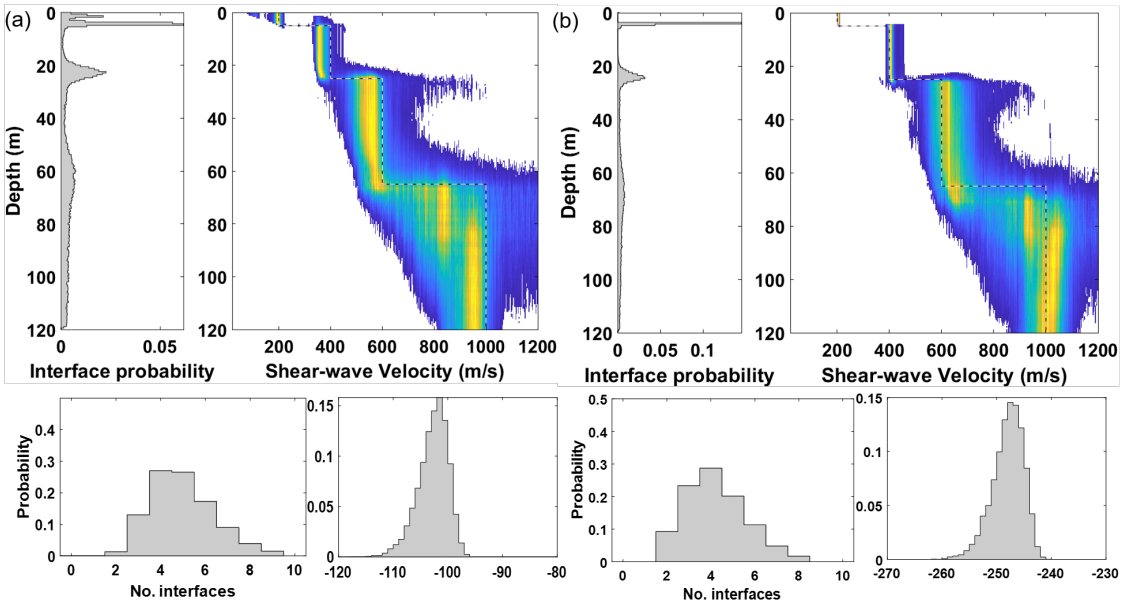

FIG. 6. (a) Vs and layer number posterior, likelihood distribution for fundamental mode. (b) Vs and layer number posterior, likelihood distribution for multimode.

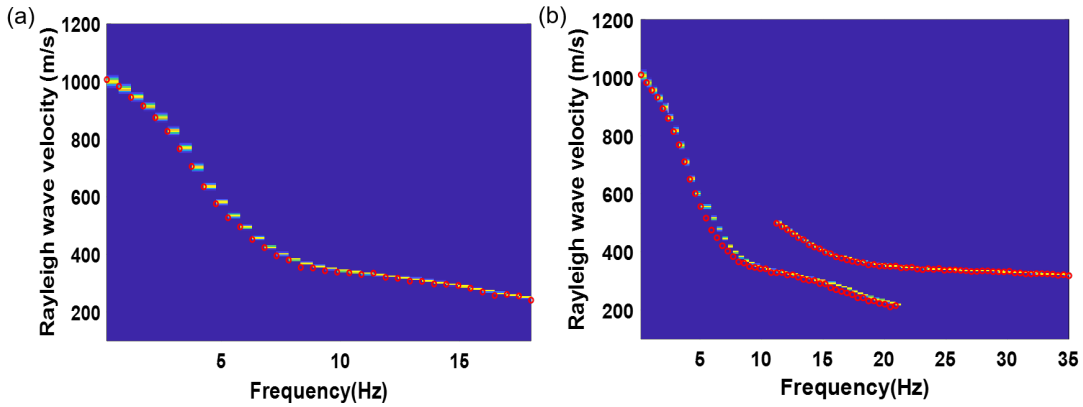

FIG. 7. Data prediction using Markov Chain samples (red dots are observing data). (a) Fundamental mode data prediction. (b) Multimode data prediction.

benefits of multimode inversion. The observing data is obtained by adding random Gaussian distributed noise on it. Figure 6 reveals the posteriors. From the comparison, uncertainty in shallow layers are reduced, some blurry additional layer in the top layer of the fundamental mode result disappears in the multimode Vs marginal posterior profile. The second layer and third layer have a better resolution as well. The bottom layer with a large velocity jump is hard to resolve in principle, as the reflection coefficient is close to 1 with a whole range of large velocities having close coefficients in the propagator matrix. Bifurcation in the bottom layer could be trade off effect, which reveals several different models could have similar dispersion curves. This inversion result shows more general solutions due to the limited information contained in dispersion curves. Besides, a better characterization of interfaces are shown in the multimode result. The interface between the third layer and fourth layer is confined to be more close with the real interface with additional mode constraint. From the data prediction using Markov Chain samples(Figure7), both the fundamental mode and

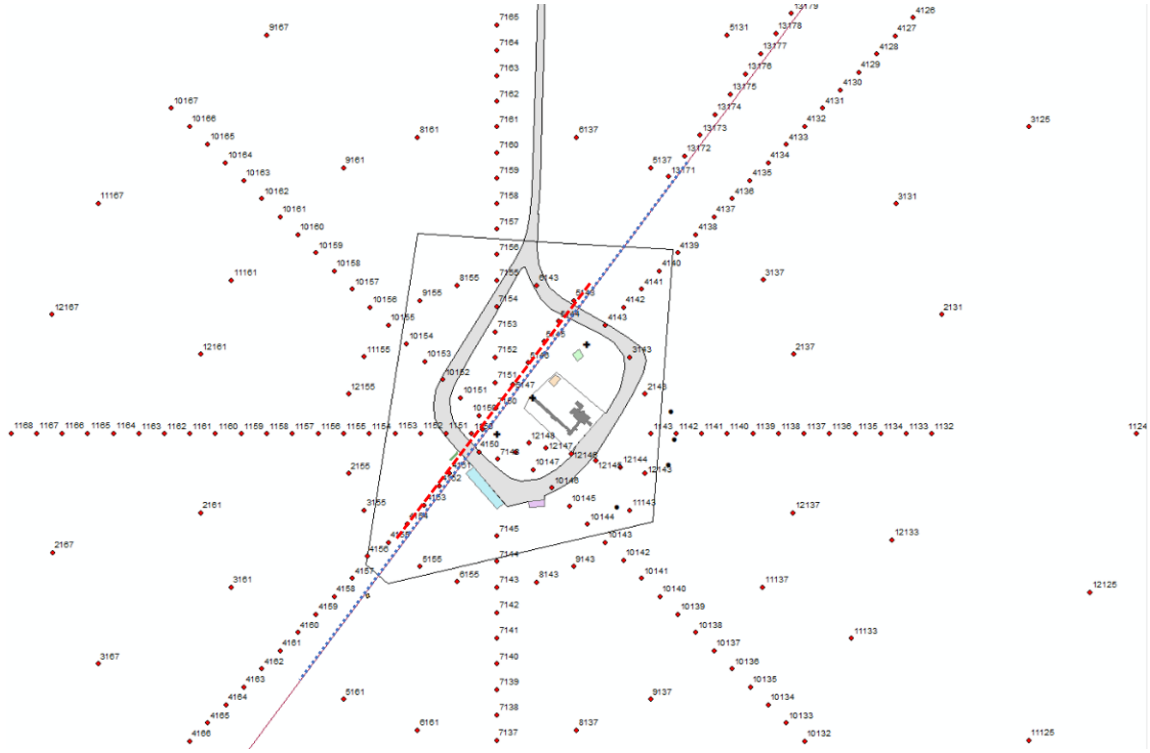

FIG. 8. Geometry for two DAS data. Red line is the fibre. Blue dotted line is the source line for first DAS data. Red dashed line is the source line for the second DAS data (Hall and Lawton, 2019).

multimode data are fitted well.

Overall, from the inversion results compared in Figure 6, multimode inversion result indicates well-defined near surface structure and substantially narrower uncertainty at all depth. The deep layer velocity is more accurately characterized compared with the fundamental mode inversion, uncertainty at shallow layers is reduced with more data constraints.

APPLICATION TO DAS DATA FROM CAMI-FRS

Data analysis

The study in this paper investigates the DAS data acquisition by active seismic source component. A straight-line fibre buried in the 1 meter deep trench with the length of 1111.4m is selected for data processing. The source used for acquisition was an IVI Enviro Vibe with a linear sweep from 1Hz to 150Hz with 2s of listening time(Hall and Lawton, 2019). The recording fibre has a nominal gauge length of 10m and trace spacing of 0.66m. Another helical fibre lying close to the straight-line fibre has the same length of 1111.4m, and the trace spacing of this fibre is 0.59m due to a pitch angle of 28.5 °. Based on previous exploration and well drilling information at this site, the near-surface geology at FRS is extremely unconsolidated and stratified. A coal layer with approximate 25 meter depth lies above the baserock. From shot record and f-k analysis of the DAS data, strong energy of multimodal ground roll could be seen, while reflection and refraction waves can hardly be observed.

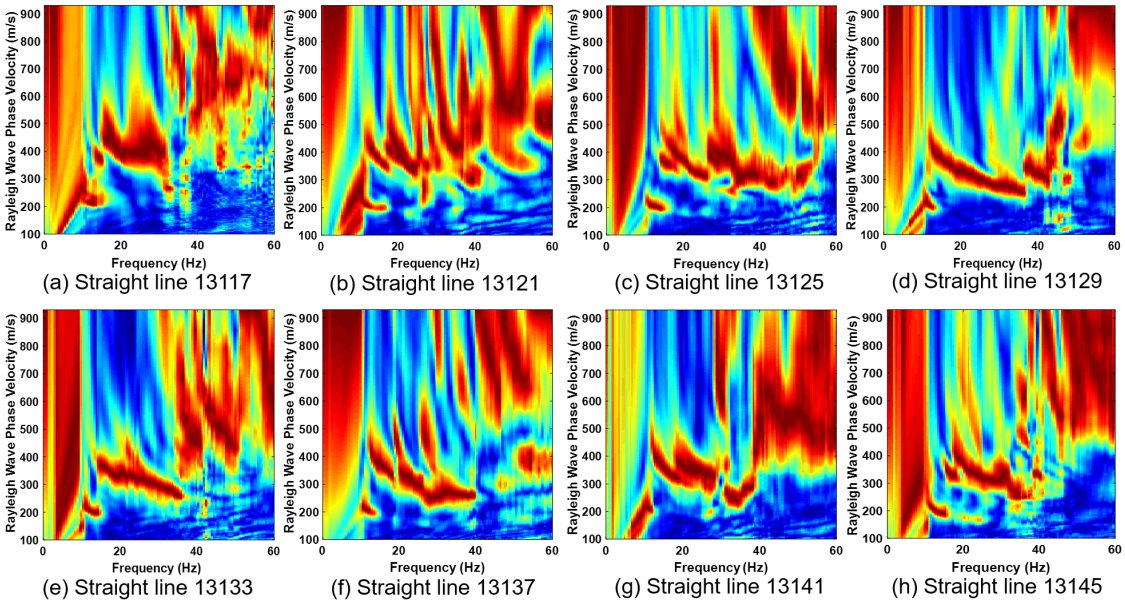

FIG. 9. Data spectrum analysis for different shots of the first DAS data.

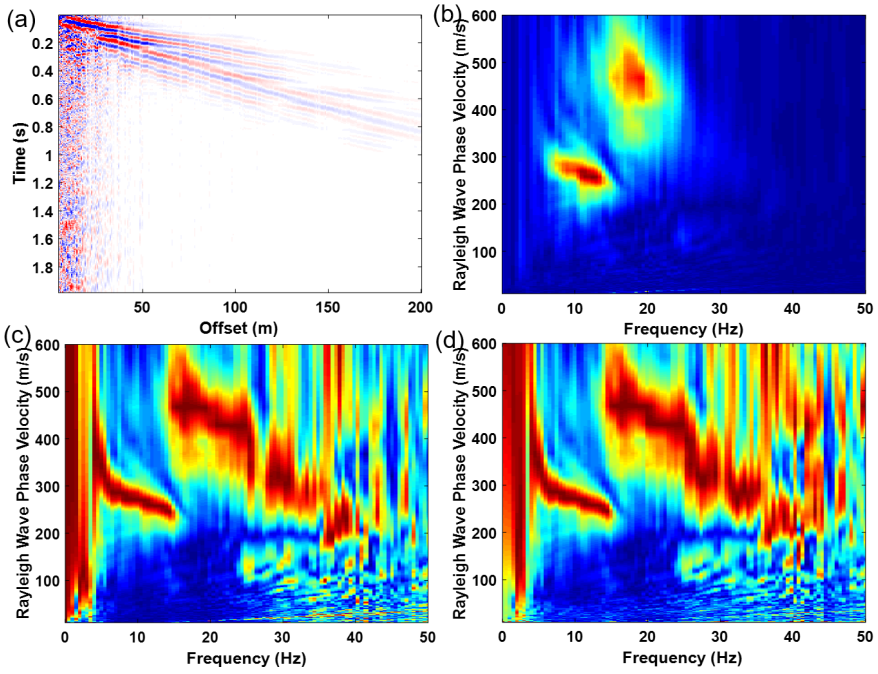

FIG. 10. Single shot record and spectrums of the second DAS data. (a) Shot record. (b) Spectrum without normalization. (c) Spectrum with normalization. (d) Spectrum with windowing normalization.

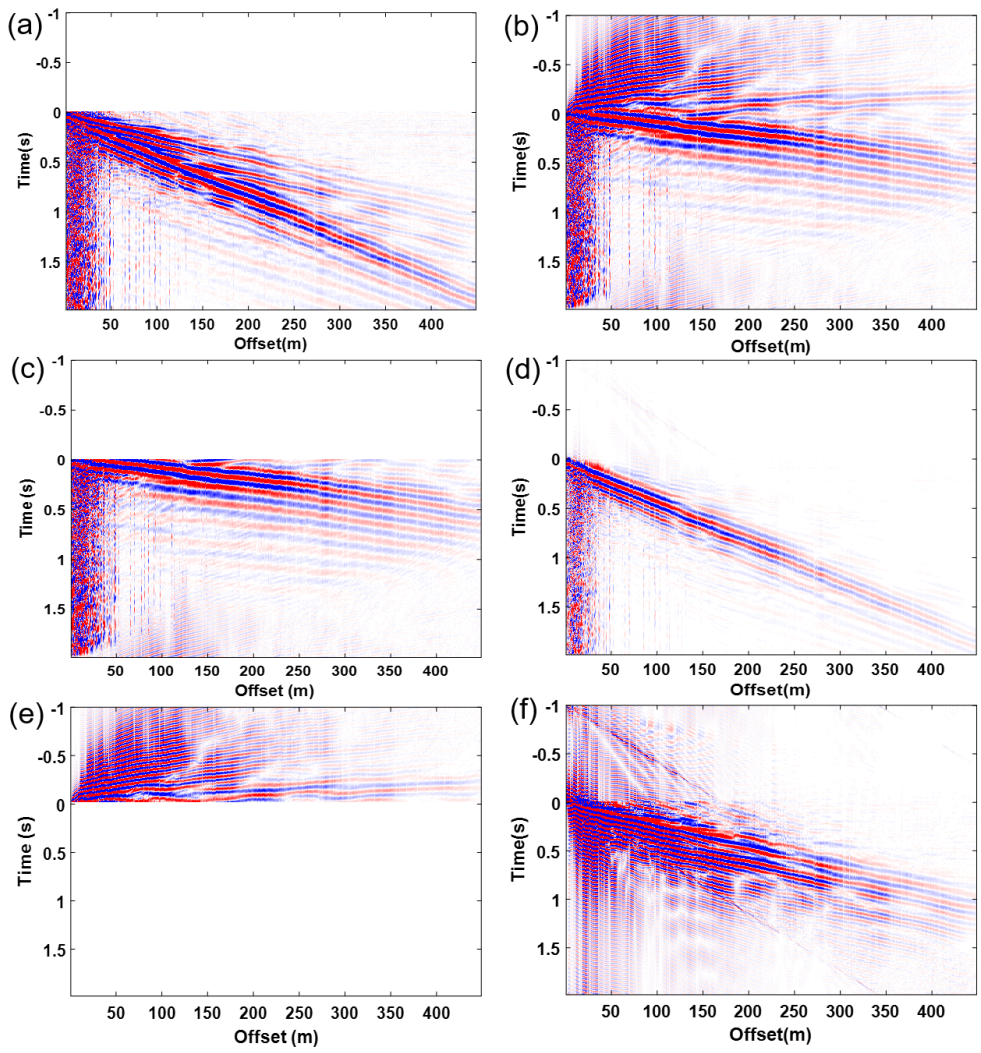

FIG. 11. Dispersion compensation. (a) Original record. (b) Record after compensation. (c) Muting higher velocity part. (d) Fundamental mode after muting. (e) Muting lower velocity part. (f) Higher modes after muting.

There are two sets of active source DAS data available at CaMI-FRS(Figure 8). The first one is a 1m deep straight line fiber trench data. It has 38 shots totally, and the sources are placed inline with the fibre. Due to the source frequency limit, it's hard to extract much useful information below 10Hz, shown in Figure 9, which will correspondingly constrain the investigation depth of Rayleigh wave. The data quality of second one is much better. It has the same receiver sets, while the source sweeps from 1Hz to 150Hz. From the spectrum of one shot data shown in Figure 10, we could find, obviously, the second data has wider frequency range, and contains richer information. Thus, we will conduct surface wave dispersion inversion on the second data. This inversion algorithm is applied to one shot of the DAS data, as these shots all have the same receivers. The frequency spectrum is obtained through $\tau - p$ transform and Fourier transform on the raw data. Multimodal specturms are displayed in Figure 10 with column normalization and windowing normalization. Then the dispersion compensation method is adopted to separate different modes in the frequency spectrum(Fig.11). 36 points(4.5Hz to 22Hz) from fundamental mode and 13 points(6Hz to

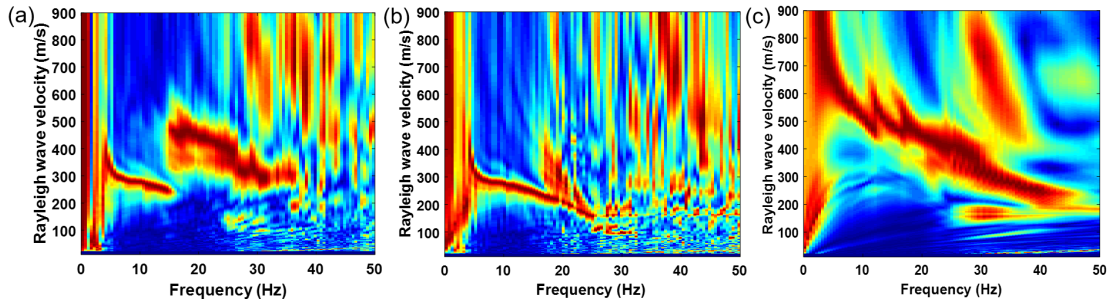

FIG. 12. DAS data multimode separation. (a) Original data spectrum. (b) Fundamental mode after separation. (c) Higher modes after separation.

12Hz) from first higher mode are picked with a regular frequency interval of 0.5 Hz(Fig.12).

With the dispersion curves we picked, the maximal investigation depth for inversion is set to be 50m.

Inversion and results

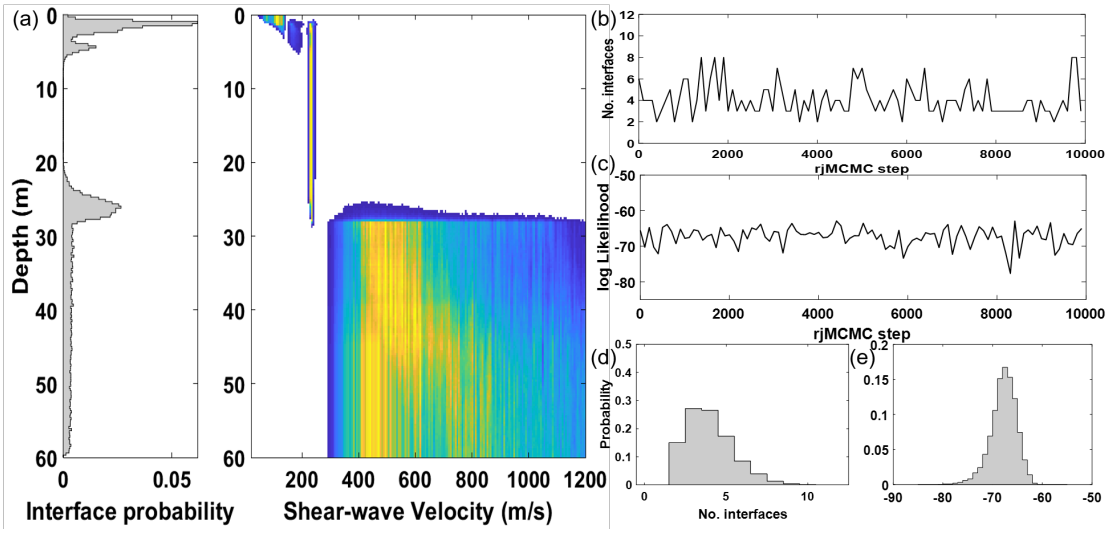

FIG. 13. Initial inversion result for DAS data. (a) Vs posterior distribution. (b) and (d) are layer number posterior distribution. (c) and (e) are likelihood distribution.

An initial inversion is conducted using the fundamental mode and assuming the data errors are independent Gaussian distributed.

The PPD results are shown in Figure 13. This figure shows there are several possible low velocity layers within 30 m depth. The first layer has a velocity around 100 m/s, and layer thickness is 3-5m. The second layer has a velocity around 260m/s, and the layer thickness is approximately 25m. The velocity below 30m is uncertain, ranging from 400 to 1200m/s. As our fundamental mode data starts from 5Hz, there is not enough data information to get the accurate velocity for this depth. Data prediction ensemble is generated using Markov Chain samples, shown in Figure 14. The data could be fitted well using this model samples. Then the data errors are estimated by the approach explained in the theory part. Next, a multimode

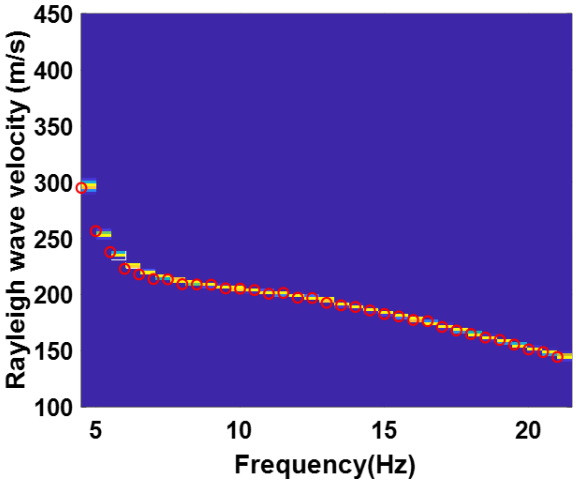

FIG. 14. Data predictions using the Markov Chain samples

inversion is conducted using fundamental mode and first higher mode. A comparison is done between inversion results obtained only using the fundamental mode and inversion results using multimode dispersion curves. Vs marginals and interface probability of multimode inversion are displayed in Figure 15.

Based on results above, there is a clear improvement in the multimode inversion results. The uncertainty of deep layer has been constrained, the uncertainty of the top layer is reduced. and the interfaces are more clear. The velocity of the bottom layer also shows the bifurcation phenomenon. Besides, data error is estimated using the data residuals with the same procedures for synthetic data, and then involved in the following inversion process. But with more constraint from first higher mode, the velocity value is more close to the real velocity value from the borehole data. For DAS data, the depth within 30 meters is well characterized with narrow uncertainty. And this result could conform the general geology structure in this field. Fundamental mode result and multimode result have close interface and velocity PPD, which further proved the result soundness.

Comparison with other studies results

This section compares our results of Vs uncertainty distribution with the shear wave velocity obtained in other studies. The first reference shear wave velocity profile is obtained through refraction migration. The second shear wave velocity profile is obtained through geophone ambient noise interferometry.

We compared out result with other results, shown in Figure 16. From the comparison, our result shows great agreements in terms of absolute velocities and interfaces. The interface at depth around 28m is the lower boundary for the coal layer matching well with borehole information. Besides, a small low velocity layer near the surface is better resolved compared with other results. This shows our method has strengths in resolving detailed structure of shallow layers and provide results easier to interpret. However, different data were used in these methods, our dispersion curve is picked from 4.5Hz, and the interferometry method

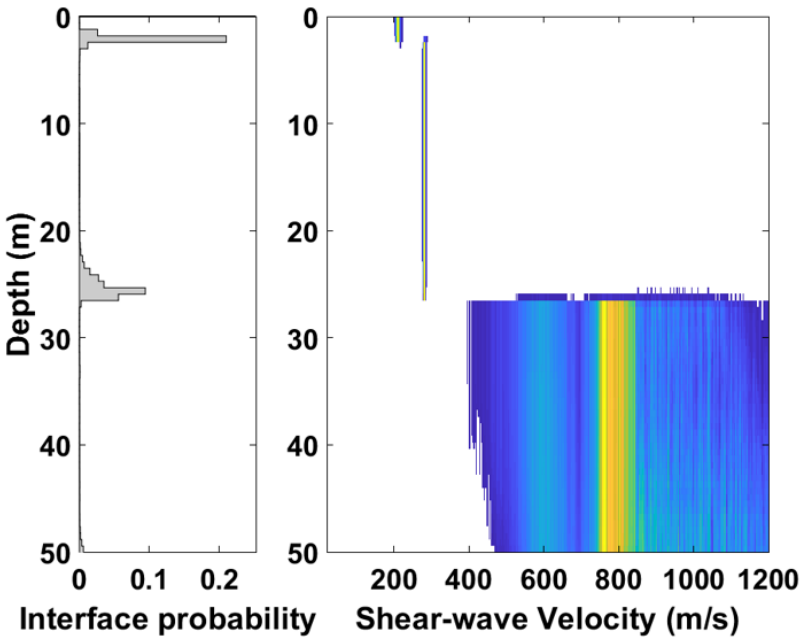

FIG. 15. Vs posterior using multimode dispersion curves

involves frequency as low as 3Hz. Therefore, it could resolve deeper layers, while the resolution ability for this DAS data extends to around 30 m. From the result, we could see there is small uncertainty within depth of 28m, which also reveals the Vs velocity model is quite robust.

CONCLUSIONS

This study focused on utilizing surface DAS data for multimode surface wave dispersion inversion. Surface DAS data provide densely sampled Rayleigh wave with no interference of other waves. Considering computational cost and geology background, an efficient and probabilistic inversion named trans-Dimensional inversion is used for quantitatively characterizing the distribution of shear wave velocity, layer thickness and layer number in shallow site. Besides, a rigorous data error estimation method is adopted to include correlated errors and non-stationary errors into the inversion process. For more efficient convergence, parallel tempering which allow dynamic state exchange between different Markov Chains and principal component rotation for better convergence are used to optimize the inversion algorithm. The inversion applied to simulated models with random data error and correlated data errors. The Vs marginal profile conforms with the true model and demonstrates reasonable uncertainty distribution. The data prediction ensemble generated by PPD samples could fit the data well. Then we applied it to multimode DAS data, and we found the result is consistent with other results. An extra low velocity layer is found from the PPD, robust shear wave velocity within 30m is obtained.

DISCUSSION

We found solution non-uniqueness when we apply the inversion algorithm on certain synthetic models. The concrete conflicts are reflected in additional lower velocity layer

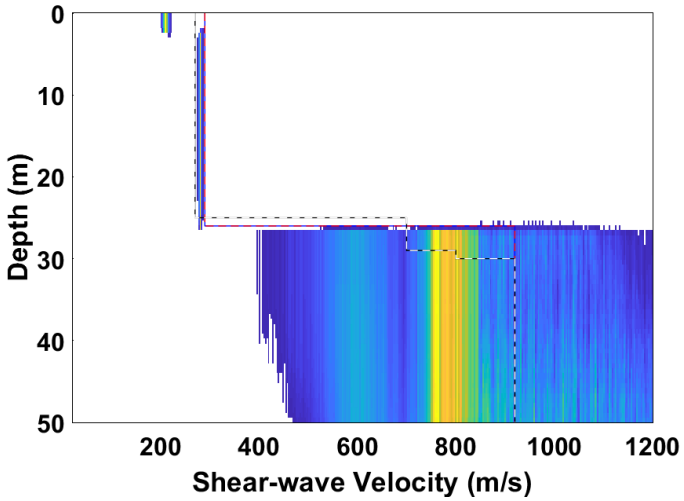

FIG. 16. Comparison with other results. (The white dashed line is the result of SWD inversion using ambient noise. The red line is the borehole velocity.)

appearing in our inversion results and models can not match with the true model appearing repeatedly in the PPD. We believe, this just reveals the trans-Dimensional inversion is quite intelligent, it explores all the possibilities that could match the dispersion curves we observed. As the forward modelling is not sensitive to low velocity layer, models with low velocity layers could be a possible model generating same dispersion curve. And since Rayleigh wave is more sensitive to root mean square (RMS) shear wave velocity due to its intrinsic characteristic, trade off models with same RMS shear wave velocity could also be the solution. And higher mode which are more sensitive to deeper parameters could help improve the result. The results shows all the models that match with certain dispersion curve, including more general posterior. We have to acknowledge the information contained in dispersion curves is limited. In order to obtain unique solution, additional data like travel time and ellipticity or priors should be incorporated as constraints. In addition, more efficient parallel tempering strategy that allow the chain block rapidly jump out of a local minimum should be explored.

ACKNOWLEDGEMENTS

We thank the sponsors of CREWES for continued support. This work was funded by CREWES industrial sponsors, NSERC(Natural Science and Engineering Research Council of Canada) through the grant CRDPJ 461179-13. Luping was partially supported by a scholarship from SEG. Thanks to the Containment and Monitoring Institute and all the field stuff for DAS data collection. Thanks also to Raul Cova for his generous sharing of surface wave data processing experience, to Zhan Niu for his helping in MPI running, to Scott Keating for his valuable suggestions on algorithms. Thanks to Don C. Lawton for providing geology information of the DAS data.

REFERENCES

Clarke, R., and Sandberg, C. L., 1983, Fiber optic temperature sensing, uS Patent 4,417,782.

Cox, B., Wills, P., Kiyashchenko, D., Mestayer, J., Lopez, J., Bourne, S., Lupton, R., Solano, G., Henderson, N., Hill, D. et al., 2012, Distributed acoustic sensing for geophysical measurement, monitoring and verification: CSEG Recorder, **37**, No. 2, 7–13.

Daley, T. M., Freifeld, B. M., Ajo-Franklin, J., Dou, S., Pevzner, R., Shulakova, V., Kashikar, S., Miller, D. E., Goetz, J., Henninges, J. et al., 2013, Field testing of fiber-optic distributed acoustic sensing (das) for subsurface seismic monitoring: The Leading Edge, **32**, No. 6, 699–706.

Dettmer, J., Dosso, S. E., and Holland, C. W., 2007, Uncertainty estimation in seismo-acoustic reflection travel time inversion: The Journal of the Acoustical Society of America, **122**, No. 1, 161–176.

Dettmer, J., Dosso, S. E., and Holland, C. W., 2010, Trans-dimensional geoacoustic inversion: The Journal of the Acoustical Society of America, **128**, No. 6, 3393–3405.

Dulaijan, K. A., and Stewart, R. R., 2010, Using surface-wave methods for static corrections: A near-surface study at spring coulee, alberta, *in* SEG Technical Program Expanded Abstracts 2010, Society of Exploration Geophysicists, 1897–1901.

Feng, S., Sugiyama, T., and Yamanaka, H., 2005, Effectiveness of multi-mode surface wave inversion in shallow engineering site investigations: Exploration Geophysics, **36**, No. 1, 26–33.

Hall, K. W., and Lawton, D. C., 2019, Trace location assignment for the cami.frs fibre loop, **volumn 31**.

Haskell, N. A., 1953, The dispersion of surface waves on multilayered media: Bulletin of the seismological Society of America, **43**, No. 1, 17–34.

Hornman, J., 2017, Field trial of seismic recording using distributed acoustic sensing with broadside sensitive fibre-optic cables: Geophysical Prospecting, **65**, No. 1, 35–46.

Krohn, D. A., MacDougall, T., and Mendez, A., 2014, Fiber optic sensors: fundamentals and applications: Spie Press Bellingham, WA.

Lawton, D. C., Osadetz, K. G., and Saeedfar, A., 2017, Monitoring technology innovation at the cami field research station, brooks, alberta: Geoconvention Slides 2017.

Li, C., Dosso, S. E., Dong, H., Yu, D., and Liu, L., 2012, Bayesian inversion of multimode interface-wave dispersion from ambient noise: IEEE Journal of Oceanic Engineering, **37**, No. 3, 407–416.

Luo, Y., Xia, J., Liu, J., Liu, Q., and Xu, S., 2007, Joint inversion of high-frequency surface waves with fundamental and higher modes: Journal of Applied Geophysics, **62**, No. 4, 375–384.

Luo, Y., Xia, J., Miller, R. D., Xu, Y., Liu, J., and Liu, Q., 2009, Rayleigh-wave mode separation by high-resolution linear radon transform: Geophysical Journal International, **179**, No. 1, 254–264.

Maraschini, M., Ernst, F., Foti, S., and Socco, L. V., 2010, A new misfit function for multimodal inversion of surface waves: Geophysics, **75**, No. 4, G31–G43.

Mateeva, A., Lopez, J., Potters, H., Mestayer, J., Cox, B., Kiyashchenko, D., Wills, P., Grandi, S., Hornman, K., Kuvshinov, B. et al., 2014, Distributed acoustic sensing for reservoir monitoring with vertical seismic profiling: Geophysical Prospecting, **62**, No. 4, 679–692.

Pan, L., Chen, X., Wang, J., Yang, Z., and Zhang, D., 2018, Sensitivity analysis of dispersion curves of rayleigh waves with fundamental and higher modes: Geophysical Journal International, **216**, No. 2, 1276–1303.

Rix, G. J., Lai, C. G., and Foti, S., 2001, Simultaneous measurement of surface wave dispersion and attenuation curves: Geotechnical Testing Journal, **24**, No. 4, 350–358.

Takeuchi, H., and Saito, M., 1972, Seismic surface waves: Methods in computational physics, **11**, 217–295.

Xia, J., Miller, R. D., and Park, C. B., 1999, Estimation of near-surface shear-wave velocity by inversion of rayleigh waves: Geophysics, **64**, No. 3, 691–700.

Xu, K., Ta, D., Moilanen, P., and Wang, W., 2012, Mode separation of lamb waves based on dispersion compensation method: The Journal of the Acoustical Society of America, **131**, No. 4, 2714–2722.